ARTICLE

Check for updates

Climate benefit of a future hydrogen economy

Didier Hauglustaine [1✉], Fabien Paulot [2], William Collins [3], Richard Derwent[4], Maria Sand[5] & Olivier Boucher[6]

Hydrogen is recognised as an important future energy vector for applications in many sectors. Hydrogen is an indirect climate gas which induces perturbations of methane, ozone, and stratospheric water vapour, three potent greenhouse gases. Using data from a state-of-the-art global numerical model, here we calculate the hydrogen climate metrics as a function of the considered time-horizon and derive a 100-year Global Warming Potential of 12.8 ± 5.2 and a 20-year Global Warming Potential of 40.1 ± 24.1. The considered scenarios for a future hydrogen transition show that a green hydrogen economy is beneficial in terms of mitigated carbon dioxide emissions for all policy-relevant time-horizons and leakage rates. In contrast, the carbon dioxide and methane emissions associated with blue hydrogen reduce the benefit of a hydrogen economy and lead to a climate penalty at high leakage rate or blue hydrogen share. The leakage rate and the hydrogen production pathways are key leverages to reach a clear climate benefit from a large-scale transition to a hydrogen economy.

[1] Laboratoire des Sciences du Climat et de l'Environnement (LSCE), CEA-CNRS-UVSQ, Université Paris-Saclay, Gif-sur-Yvette, France. [2] Geophysical Fluid Dynamics Laboratory, National Oceanic and Atmospheric Administration, Princeton, NJ, USA. [3] Department of Meteorology, University of Reading, Reading, UK. [4] rdscientific, Newbury, UK. [5] Center for International Climate and Environmental Research—Oslo (CICERO), Oslo, Norway. [6] Institut Pierre-Simon Laplace (IPSL), Paris, France. ✉email: didier.hauglustaine@lsce.ipsl.fr

Molecular hydrogen (H_2) is increasingly presented as a key element of the worldwide energy transformation required to limit global warming and meet the Paris Agreement[1] climate objectives. H_2 is recognised as an important future energy vector for applications ranging from power generation, transportation, industry, building heating and energy storage[2–8]. The use of hydrogen produced by a renewable source of electricity enables the conversion and the storage of energy, and may provide a way to decarbonize sectors of the economy difficult to decarbonize such as long-distance transportation by trucks and airplane, heavy industries, or for domestic uses blended with natural gas[4].

H_2 is a symmetric molecule with no direct impact on infrared radiation at temperature and pressure conditions prevailing in the Earth's atmosphere[9]. However, hydrogen is recognized as an indirect greenhouse gas through its involvement in chemical reactions which affect the lifetime and concentration of other greenhouse gases[10,11]. In particular, tropospheric oxidation of H_2 depletes the hydroxyl radical (OH). Since OH is the main sink for methane, a potent greenhouse gas, this results in a lengthening of the methane atmospheric lifetime. H_2 and methane are also precursors of tropospheric ozone and a photochemical source of water vapour in the dry stratosphere[12,13], both of which also act as greenhouse gases.

Firn air measurements from South Pole indicate that the concentration of hydrogen has increased from about 350 parts per billion (ppbv) in 1910 to about 540 ppbv in 2000[14]. Today, the sources of H_2 are oxidation of methane and other hydrocarbons in the atmosphere (56%), fossil fuel combustion (23%), biomass burning (12%), and nitrogen fixation in the soils and ocean (12%)[15]. Hydrogen is removed from the atmosphere by oxidation by OH (about 25%) and by soil uptake due to bacterial activity (about 75%)[15]. The burden of H_2 in the troposphere (136–162 Tg)[15] and its production and destruction terms are however uncertain in both magnitude and distribution[12,15–17]. In particular, the critical role played by biological H_2 soil consumption is subject to considerable differences among the various estimates (55–88 Tg/year)[15–19]. This is reflected in the large range of estimates for H_2 tropospheric lifetime (1.4–2.3 years)[12–20].

The development of a future large-scale hydrogen economy has the potential to increase the atmospheric source of H_2 through leakage during production, transport, storage and use. Based on previous reports[2,6,21], leakage rates are likely to range from 1 to 10%. Hereafter, we will refer to these leakage rate as low and high leakage rates, respectively. These fugitive hydrogen emissions were found to have minor implications for both air quality[2,21–24] and stratospheric ozone depletion[24,25], unless unrealistic leakage rates of 20%[8,26], are considered[27]. The climate impact of hydrogen is assessed in terms of the Global Warming Potential (GWP) climate metric[3,10,11,28] or more recently in terms of radiative forcing and equilibrium temperature change[15,29]. With calculated GWP_{100} of 5.0 ± 1.0[28] and 3.3 ± 1.4[3], earlier assessments indicate that the climate impact of hydrogen is relatively minor compared to other potent greenhouse gases with more important anthropogenic emissions such as carbon dioxide (CO_2), nitrous oxide (N_2O) or methane (CH_4). However, recently, the climate benefit of a hydrogen economy has come into question. A first reason is that the climate impact of a hydrogen economy depends on how hydrogen is produced. In particular the production of "decarbonized" hydrogen from oil and gas depends on capture and storage of the CO_2 produced[4,30], and on the associated upstream methane leakage[4,31–33]. Secondly, since the indirect hydrogen impact on climate involves chemical reactions in the atmosphere, the uncertainties on key processes affecting the H_2 distribution and budget hamper a precise quantification of the associated radiative forcings[13,34]. As an illustration of this uncertainty, a recent study revised the hydrogen GWP_{100} value to more than twice its previously estimated value[35]. Furthermore, GWP_{100}, the climate metric used by the United Nations Framework Convention on Climate Change (UNFCCC) when reporting emissions of different greenhouse gases, is often criticized for over- or understating the importance of Short-Lived Climate Forcers (SLCFs), like H_2[4,29,36–39].

Here, we use recent global H_2 perturbation simulations and associated radiative forcings of climate[15] to derive hydrogen climate metrics. The metrics are decomposed into their various contributions from methane, tropospheric and stratospheric ozone (O_3) and stratospheric water vapour (H_2O). Based on these metrics and on future roadmaps for transition to an hydrogen economy in Europe and worldwide, we quantify the climate benefit of such hydrogen decarbonization pathways. In particular, we illustrate the impact of a hydrogen economy on the cumulative CO_2 emissions abatement over the Paris Agreement long-term climate goal.

Results

Hydrogen climate metrics. The H_2 radiative forcings (Effective Radiative Forcings, ERFs) used in this study are taken from the global chemistry-climate model GFDL-AM4.1[40] simulations[15]. Based on these simulations and modelling set-up[15], a H_2 total radiative efficiency (i.e., ERF per ppbv increment) of $0.13 \, mW \, m^{-2} \, ppbv^{-1}$ was calculated. This radiative efficiency was further decomposed into a methane efficiency (46% or $0.0598 \, mW \, m^{-2} \, ppbv^{-1}$), a stratospheric H_2O efficiency (28% or $0.0364 \, mW \, m^{-2} \, ppbv^{-1}$), a tropospheric ozone efficiency (21% or $0.0273 \, mW \, m^{-2} \, ppbv^{-1}$), and a stratospheric ozone efficiency (5% or $0.0065 \, mW \, m^{-2} \, ppbv^{-1}$). These radiative efficiencies were derived from a steady-state perturbation to a sustained 200 TgH_2/year emission[15]. This perturbation is likely an upper bound for future emissions[15], however we only use these results as radiative efficiencies (i.e., on a per ppbv basis) and will apply future H_2 emission scenarios as a subsequent step. The H_2 total indirect radiative efficiency relative to the CO_2 radiative efficiency of $1.33 \times 10^{-5} \, W \, m^{-2} \, ppbv^{-1}$ (calculated based on the CO_2 ERF and 2019 background concentrations[41]), on a kg per kg basis, is 215. On a mass basis, the radiative impact of H_2 is larger than those of CH_4 (118) and N_2O (210) but smaller than those of halogenated compounds such as CFC11 (7679) or CFC12 (8694)[41]. The radiative impact of H_2 is significant compared to other potent greenhouse gases. However, what really matters for climate is the integrated energy absorbed by the system. Hence, the lifetime of the considered greenhouse gas is a key parameter to consider and H_2 has a short lifetime of 2.5 years in the whole atmosphere (or 2.1 years in the troposphere)[15] compared to decade(s) or even centuries in the case of CH_4, CFC11, CFC12, N_2O, and CO_2.

Future hydrogen demand levels reaching up 3000 TgH_2/year were recently applied to derive an equilibrium global surface temperature increase[29]. However, the climate steady-state to a perturbation in hydrogen emissions will be reached over centuries, providing that all other parameters are constant. In order to quantify the climate impact of H_2, it is essential to consider the transient behaviour of the perturbation. In particular, other climate metrics are required to effectively estimate the climate impact of a transition to a hydrogen economy during the next 75 years. The two most commonly used climate metrics are the GWP and the Global Temperature Potential (GTP)[42–44]. The GWP is the time-integrated radiative forcing due to a pulse of emission, over a given time-horizon relative to an equal mass pulse of CO_2. In order to better represent the actual impact of a greenhouse gas on the global-mean surface temperature, the GWP concept has been extended to the GTP metric which provides the temperature effect of a gas
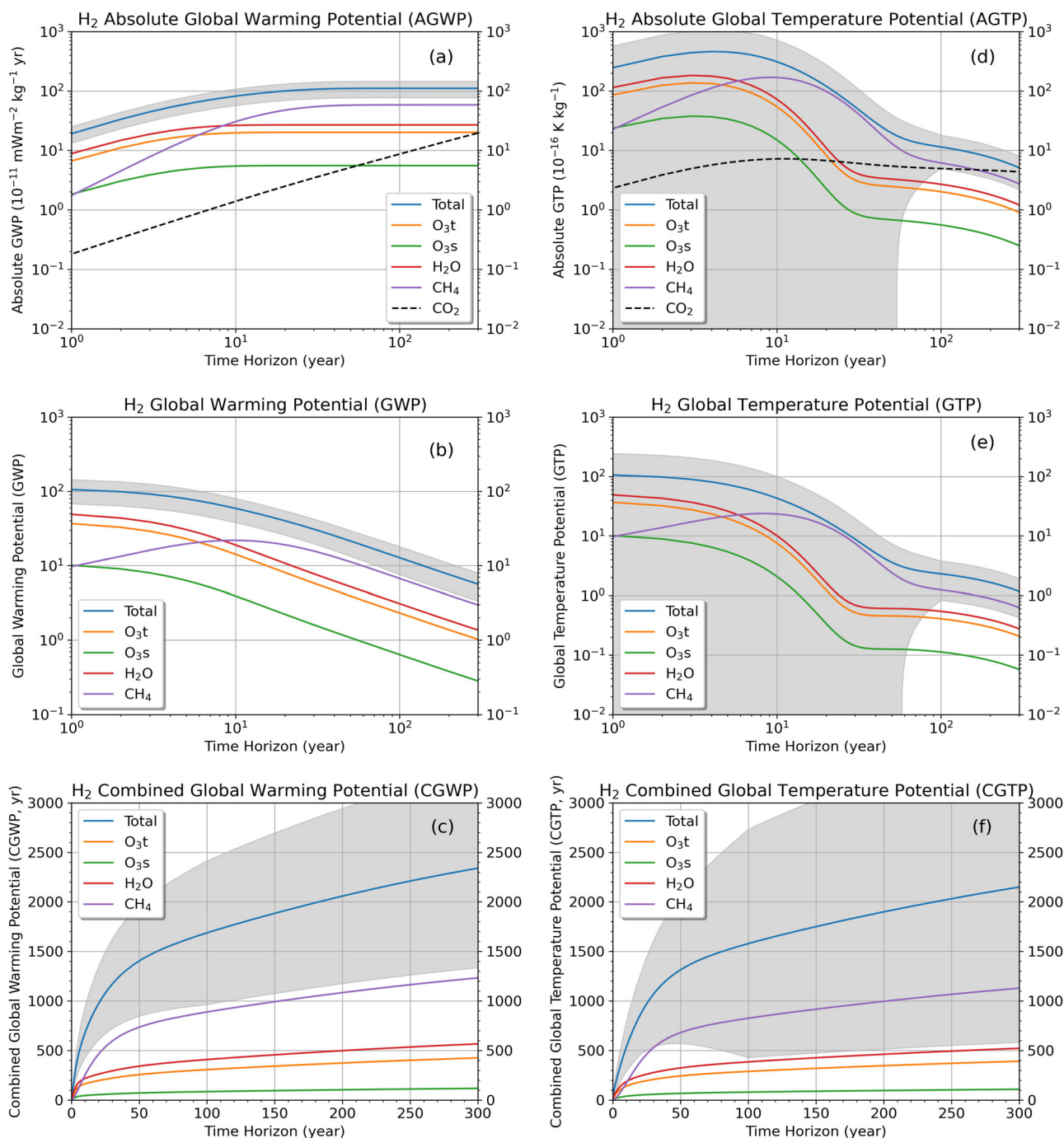
Fig. 1 Hydrogen climate metrics as a function of the considered time horizon. a Absolute GWP (AGWP, in 10^{-14} W/m^2/kg year) and **d** Absolute GTP (AGTP, in 10^{-16} K/kg); **b** GWP (unitless) and **e** GTP (unitless); and **c** CGWP (year) and **f** CGTP (year) for hydrogen as a function of time-horizon. The total metrics (blue solid line) are decomposed into their tropospheric ozone (O_3t), stratospheric ozone (O_3s), stratospheric water vapour (H_2O), and methane (CH_4) components (see legend for colouring). The metrics are calculated for a pulse emission of 1 Tg of hydrogen. The AGWP and AGTP for CO_2 are also illustrated for comparison. Uncertainty calculations are presented in Supplementary Table S2 and 90% confidence level are represented as a shaded area for the total metrics.

emission at a given time-horizon[42]. The GWP and GTP of H_2 are calculated as a function of the time-horizon, based on the radiative efficiencies[15]. An uncertainty analysis for these different metrics based on the IPCC methodology[41] has been performed (details are available in the "Methods" section).

Figure 1a shows the Absolute GWP (AGWP) calculated for H_2 and decomposed into its different contributions. Rather than focusing on a particular time-horizon, we estimate and show the AGWP as a function of the time-horizon. The total AGWP

increases with the time-horizon, reaching a maximum value of $1.11 \pm 0.34 \times 10^{-12}$ W/m^2/kg year about 20 years after emission. The indirect AGWP associated with ozone and stratospheric H_2O reach a maximum after 8 years. The indirect AGWP of methane shows a different time-scale and increases over a period of about 30 years. This shows the importance of decomposing the H_2 indirect forcing into a short-term component characterized by the H_2 lifetime and a longer-term component characterized by the methane perturbation lifetime of 12.4 years[43]. As shown on this

Table 1 GWP, GTP, CGWP, and CGTP metrics for hydrogen at 20, 40 and 80 and 100-year time-horizons.

	20 year	40 year	80 year	100 year
GWP	40.1 ± 24.1 (33.8 ± 12.2)	25.3 ± 9.4 (21.2 ± 7.9)	15.1 ± 6.0 (12.7 ± 5.0)	12.8 ± 5.2 (10.7 ± 4.4)
GTP	17.8 ± 23.3 (14.1 ± 18.5)	5.1 ± 5.8 (4.2 ± 4.7)	2.5 ± 2.0 (2.1 ± 1.7)	2.3 ± 1.5 (1.9 ± 1.2)
CGWP	973 ± 370 (820 ± 312)	1304 ± 512 (1094 ± 430)	1594 ± 666 (1336 ± 558)	1687 ± 725 (1413 ± 607)
CGTP	852 ± 596 (723 ± 340)	1213 ± 652 (1019 ± 548)	1496 ± 999 (1254 ± 838)	1579 ± 1153 (1324 ± 966)

Metrics are unitless by definition except for CGWP and CGTP (year). The values calculated based on the northern hemisphere hydrogen lifetime are provided under parenthesis. Uncertainty calculations are presented in Supplementary Table S2 and 90% confidence levels are provided here.

figure, even after 300 years, the CO_2 AGWP is still increasing, stressing the importance of considering the difference in lifetime between the short-lived H_2 forcing and the long-term CO_2 forcing. Figure 1b shows the resulting total hydrogen GWP and its individual components as a function of the considered time-horizon. The evolution and decrease of the GWP with the time-horizon after 3 years is controlled by the increase of the CO_2 AGWP as seen in Fig. 1a. The H_2 GWP decreases from a value of 106 ± 38 for a very short-time horizon (GWP_1) to a value of 40.1 ± 24.1 for a 20-year time-horizon (GWP_{20}) and 12.8 ± 5.2 for the 100-year time-horizon (GWP_{100}) (Table 1). The impact of H_2 on the methane lifetime and the associated GWP component shows a different temporal profile than the other short-term contributions from tropospheric and stratospheric ozone and stratospheric H_2O, and peaks at a time-horizon of 10 years. The methane contribution represents 48 and 53% of the H_2 GWP_{20} and GWP_{100}, respectively (Supplementary Fig. S1a, b). The H_2 GWP_{100} is larger than the earlier estimate of 5.8 with the STOCHEM three-dimensional model[10,11], the value of 5.0 ± 1.0 recalculated with the same model[28], and with the value of 3.3 ± 1.4 calculated with the TROPOS two-dimensional model[3]. This discrepancy can be attributed to a higher methane radiative efficiency[45], to the indirect effects of stratospheric H_2O and stratospheric ozone not included in the previous estimates, and to the longer H_2 tropospheric lifetime (2.1 years)[15] compared to these earlier estimates (1.6 years)[28]. This emphasizes the sensitivity of the results to assumptions made for H_2 soil uptake. Our results are consistent with a more recent estimate[35] which derived a H_2 GWP_{100} of 11 ± 5 using a state-of-the-art global climate-chemistry model.

The calculated Absolute GTP (AGTP) of H_2 is illustrated as a function of the time-horizon in Fig. 1d. The AGTP shows a short-term increase and peaks after 4 years. The AGTP then falls down by several orders of magnitude, in line with the short timescale of the temperature change response function. This sharp decrease is then followed by a slower decrease for time-horizons >60 years where the longer time-scale of the temperature response becomes more important. The AGTP of CO_2 increases rapidly with the time-horizon before peaking after about 10 years and decreasing slowly thereafter. The resulting H_2 GTP is illustrated in Fig. 1e. The GTP decreases rapidly from a value of 106 ± 139 for a very short time-horizon to a value of 17.8 ± 23.3 for a 20-year time horizon (GTP_{20}) and 2.3 ± 1.5 for a 100-year time horizon (GTP_{100}). The longer-term methane indirect effect increases to a maximum value reached about 10 years after emission and decreases thereafter. The methane response contributes 82% to the hydrogen GTP_{20} and 54% to the GTP_{100} (Supplementary Fig. S1c, d).

Due to the larger fraction of land in the northern hemisphere than in the southern hemisphere, this results in a larger sink by soil uptake and hence a shorter atmospheric residence time of H_2 in the northern hemisphere. This contrast explains the observed H_2 enhancement in the southern hemisphere[16,20]. The H_2 global lifetime in the troposphere derived based on the GFDL-AM4.1

model simulations is 2.1 years[15]. Over the whole atmosphere this corresponds to a global atmospheric lifetime of 2.5 years. This global atmospheric lifetime is used in this study for the GWP and GTP calculations. Averaged over the northern hemisphere solely, the calculated H_2 atmospheric lifetime is 2.0 years. The shorter lifetime of H_2 in the northern hemisphere reduces the climate impact of H_2 emitted in this region ($GWP_{100} = 10.7 ± 4.4$ and $GTP_{100} = 1.9 ± 1.2$) (Table 1). These northern hemisphere values will be used hereafter to quantify the climate impact of European H_2 leakages.

The GWP and GTP climate metrics are defined in terms of a pulse emission of a species. For a SLCF such as H_2, several authors also suggested the use of metrics defined in terms of a sustained change in emissions to express equivalence between cumulative climate pollutants and SLCFs[31,42,46–48]. The 's' subscripts denote metrics based on sustained emissions. The use of a sustained emission increases the calculated GWP of H_2 after a few years and the 100-year time-horizon GWP_s is 20.8 ± 8.5, 1.6 times larger than the GWP. Sustained metrics are barely used and are essentially calculated here in order to derive the combined climate metrics (see below).

Figure 1b, e and Table 1 show that both GWP and GTP metrics vary considerably with the considered time-horizon. For a SLCF such as hydrogen, there is a scalar factor of 3.1 for the GWP and 7.7 for the GTP in the value of the metric for a 20-year versus a 100-year time-horizon. In order to reconcile the impact of cumulative climate pollutants and SLCFs, combined metrics[44] have been defined as the ratio of a sustained response of the considered SLCF to a pulse response of CO_2 (details available in the "Methods" section). These combined metrics, based on the end-point metrics GFP (Global Forcing Potential) and GTP, measure the progress towards a steady-state temperature. The combined metrics are no longer dimensionless, but have units of time, reflecting the need to compare rates (kg/year) with pulses (kg). Figure 1c show the calculated Combined GWP (CGWP) and Combined GTP (CGTP) of H_2. As shown also in Table 1, CGWP and CGTP vary less with the time-horizon and there is a scalar factor of 1.7 for the CGWP and 1.4 for the CGTP in the value of the metric for a 20-year versus a 100-year time-horizon. After about 20 years, the time variation of these metrics for a short-lived species like H_2 is essentially due to the decrease of CO_2 following the pulse emission.

Climate consequences of a future hydrogen economy. To deliver on the sustainability promise it is important to maximize the hydrogen decarbonization potential. The most common way of producing hydrogen today is by reforming natural gas into hydrogen and CO_2, which is referred to as grey hydrogen if the CO_2 is emitted into the atmosphere, or blue hydrogen if the CO_2 is captured and permanently sequestered. If renewable sources are used for water electrolysis, the hydrogen produced is referred to as green. The climate impact of a future hydrogen economy depends on the intensity of the deployment of the hydrogen

energy supply in the different sectors of the economy but also on the hydrogen production pathways.

The climate impact of an hydrogen economy also depends on the fraction of H_2 lost to the atmosphere during production, transport, storage and use through venting, fugitive emissions and incomplete combustion[5,49]. The future leakage rate of hydrogen into the atmosphere is a major uncertainty and our assessment of the climate impact of an hydrogen economy transition is performed assuming different leakage rates. In order to investigate the climate benefit of a future hydrogen powering economy, several scenarios for worldwide and European energy supply by hydrogen are considered in this study (details available in the "Methods" section). In the future, the global hydrogen production portfolio will contain a mix of both green, blue and grey hydrogen production pathways. For green hydrogen, the equivalent CO_2 emission is calculated by multiplying the total hydrogen production by a leakage fraction and by the considered climate metric for different time-horizons. The total hydrogen production is itself increased by the leakage rate in order to meet the given supply. For grey and blue hydrogen, in addition to this CO_2 equivalent emission associated with the H_2 leakage rate, we add carbon dioxide and methane emissions (details available in the "Methods" section).

We first evaluate the carbon-saving potential of an installed 2050 worldwide hydrogen economy based on scenario HC2017 for global decarbonization and hydrogen supply (See "Methods" for a brief description of the HC2017 scenario proposed by the Hydrogen Council in 2017[50,51]). The climate benefit in 2050 is determined by dividing the hydrogen CO_2 equivalent emissions, calculated based on the chosen climate metric and time-horizon, by the avoided CO_2 annual emission. According to scenario HC2017, in 2050, hydrogen provides worldwide some 21,667 TWh (78 EJ), an almost eight-fold increase of hydrogen consumption over the 2020–2050 period. Such an energy production from hydrogen is estimated to abate the CO_2 emissions by 6 GtCO$_2$/year[50]. This abatement corresponds to 10.9 kgCO$_2$ avoided per kgH$_2$ across all energy supply sectors. Figure 2 shows the percentage of remaining carbon equivalent emissions considering an hydrogen economy as a function of the metric time-horizon and assumed leakage rate. We illustrate the climate impact of an hydrogen economy assuming an optimistic case of 100% green hydrogen supply, or a mix of blue + green hydrogen. Figure 2a provides the climate benefit assuming a green hydrogen economy and based on the GWP climate metric. By definition, no leakage of green hydrogen would provide 0% of CO_2 equivalent emission. When a very low leakage rate of 0.1% is assumed, the H_2 emission to the atmosphere represents 0.1% of the abated CO_2 emission based on the GWP$_{100}$. In this case, 99,9% of the fossil fuel based CO_2 emissions are avoided. Using a shorter time-horizon (GWP$_{20}$), increases the CO_2 equivalent emissions to 0.4% (a 99.6% benefit in terms of avoided CO_2 emissions). In contrast, in the case of a high leakage rate of 10%, the CO_2 equivalent emissions represent about 13% of the abated CO_2 emissions for a 100 year time-horizon (about 40% at a 20 year time-horizon). It is only for leakage rates of 10 and 15%, and at a very short time-horizon of 1 year (not realistic from a climate pespective) that the hydrogen economy results in a climate penalty, reaching 167% (CO_2 equivalent emissions higher than the abated emissions by 67%). In the case of a mix of blue + green hydrogen (assuming, according to the 2050 HC2017 scenario, 30% of blue hydrogen and 70% of green hydrogen), the CO_2 equivalent emissions increase and represent 20.1% (resp. 28.3%) of the abated emissions for a 100 year (resp. 20 year) time-horizon and a 1% leakage rate, and represent 64% (resp. 153%) for a 10% leakage rate (Fig. 2b). In a mix of blue + green hydrogen supply, equivalent CO_2 emissions increase

strongly with the hydrogen (and methane) leakage rate and largely offset the climate benefit of the hydrogen economy. At a high leakage rate of 10%, the equivalent CO_2 emissions represent 64.5% of the abated CO_2 emissions at a 100 year time-horizon but 153.3% of the abated emissions at a 20-year time-horizon. This moderate climate benefit obtained in the case of a mix of blue + green hydrogen strongly depends on the assumed blue hydrogen supply. For a 1% leakage rate, the equivalent CO_2 emissions associated with an hydrogen economy increase to 26.5%, 32.8%, 39.1% and 51.7% at a 100 year time-horizon for a 40%, 50%, 60 and 80% fraction of blue hydrogen (Fig. 3). It shows that, based on the GWP$_{100}$, a portfolio composed of >60% of blue hydrogen has basically no climate benefit if the leakage rate is >7%. Based on the GWP$_{20}$, the climate benefit is lost if the blue hydrogen fraction is >30% and if the leakage rate exceeds 3%. In the case of a green hydrogen supply, the use of GWP$_s$ increases the CO_2 equivalent emissions by a factor of 1.3 and 1.6 for a 20 year and 100 year time-horizon, respectively, independently of the leakage rate (Supplementary Fig. S2). In the case of a blue + green supply, this ratio between GWP$_s$ and GWP based equivalent emissions depends on the leakage rate and is reduced compared to the green hydrogen case since a fraction of the equivalent CO_2 emission is associated with the methane leakage. With a lifetime longer than H_2, the CH_4 GWP$_s$ is less affected than H_2 by the use of the sustained metric at longer time-horizons (Supplementary Fig. S3).

In order to illustrate the sensitivity of the results to the hydrogen technologies, the calculations were repeated using the hydrogen Lower Heating Value (LHV) instead of the Higher Heating Value (HHV) used in previous studies[3,4,11,50] (details available in the "Methods" section). Assuming the LHV implies that about 18% more hydrogen needs to be produced in order to supply the same energy. In the case of a green hydrogen economy, when a low leakage rate of 1% is assumed, the hydrogen CO_2 equivalent emissions increase from 1.2% with the HHV to 1.4% with the LHV based on the GWP$_{100}$. In the case of a high leakage rate of 10%, the CO_2 equivalent emissions increase from 13% with the HHV to 15% with the LHV for a 100 year time-horizon (Supplementary Fig. S4a). In the case of a mix of blue + green hydrogen, the CO_2 equivalent emissions increase from 20% with the HHV to 24% with the LHV for a 1% leakage rate and from 64% with the HHV to 76% with the LHV for a 10% leakage rate (Supplementary Fig. S4b).

Unlike the GWP, the GTP quantifies the climate effect at the end of a timeperiod rather than averaging over the whole timeperiod. The GTP therefore gives more weight to the radiative forcing that comes later in the timeperiod. Whereas, using a GWP to trade a short-lived species like H_2 against the long-lived like CO_2 tends to overestimate the importance of H_2 for reaching long-term climate goals[42,52]. If Article 2 of the Paris Agreement is interpreted as a long-term climate goal, the GTP appears as an appropriate metric to use. When the GTP is used, the CO_2 equivalent emissions associated with H_2 are reduced and represent <5% of the abated emissions for a time-horizon in the range 20–100 year and a 1–3% leakage rate in the case of a green hydrogen economy (Fig. 2c). More generally, in the case of a green hydrogen supply, the use of the GWP instead of the GTP increases the CO_2 equivalent emissions by up to a factor of 6.2 for a 75 year time-horizon (Supplementary Fig. S5). In the case of a blue + green hydrogen supply, this ratio between GWP and GTP emissions depends on the leakage rate and is reduced to less than a factor of 4 reflecting the role of the leaks on the longer-lived methane (Supplementary Fig. S6).

We now calculate the cumulative CO_2 abatement resulting from the transition to an hydrogen economy over the entire 2030–2100 period. We use the HC2017 scenario for the 2030, 2040 and 2050 decades and assume 2050 values for decades
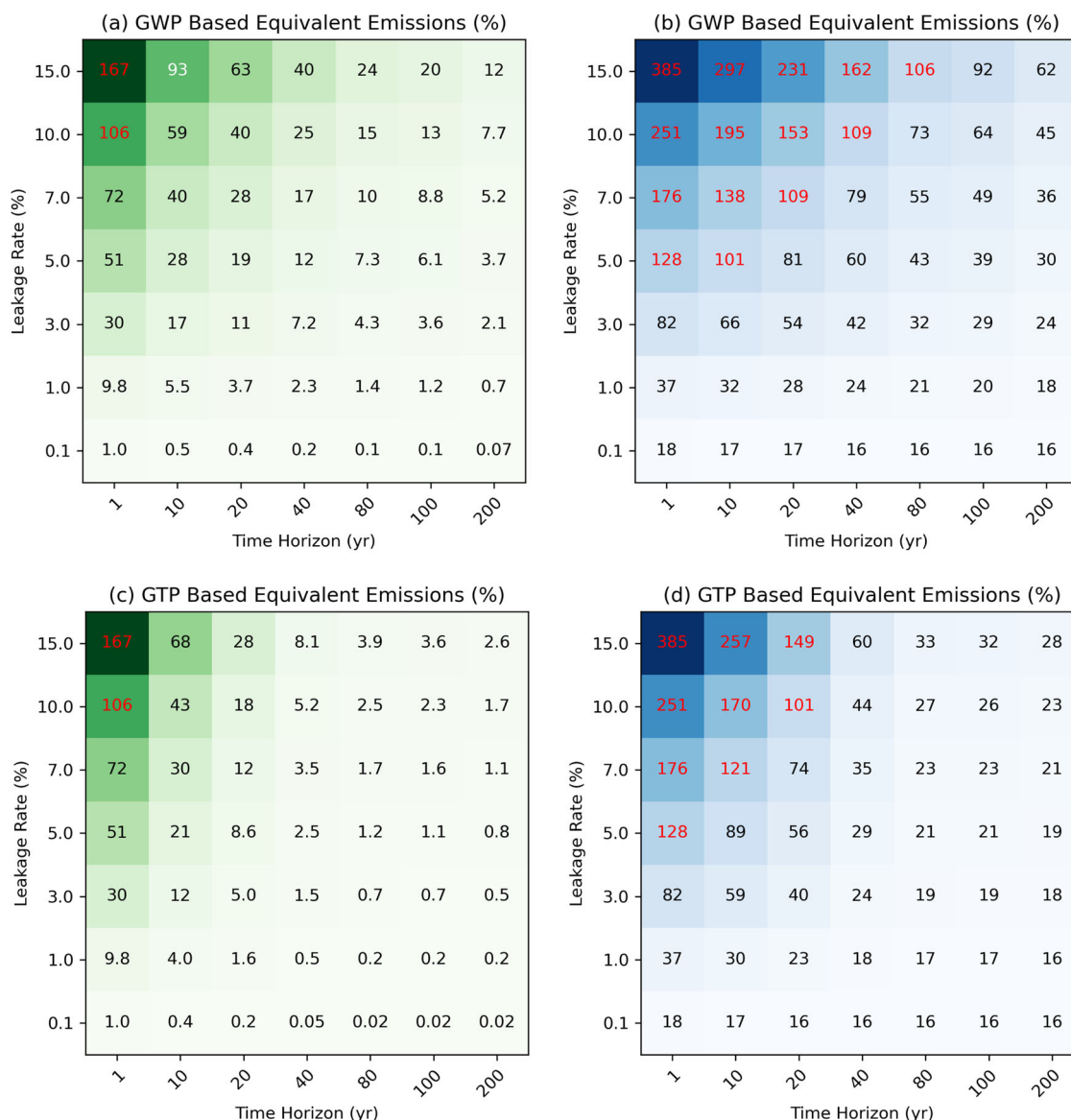
Fig. 2 Climate benefit of a global energy transition to hydrogen. Ratio (expressed in %) of CO_2 equivalent emissions associated with a hydrogen economy to the avoided CO_2 emissions as a function of the hydrogen leakage rate and the metric time-horizon. **a, b** GWP based emission ratios, **c, d** GTP based emission ratios. The emission ratios are calculated assuming a green hydrogen supply only (left) and assuming blue + green hydrogen with a 30% blue hydrogen supply as assumed in the HC2017 scenario for 2050 (right). The net climate penalty conditions (ratios > 100%) are provided.

thereafter. We add the CO_2 or H_2 emissions over the entire 2030–2100 period in order to calculate the cumulative emissions needed to supply the same energy over the full period. For this given energy supply scenario, we compare the CO_2 emissions abated due to a greater use of hydrogen in the economy (i.e., the emissions that would have resulted from a business-as-usual fossil-fuel based economy without hydrogen) and the hydrogen equivalent CO_2 (CO_2e) emissions released into the atmosphere to supply the same energy. For the full period, this scenario results in a total abatement of CO_2 emissions worldwide by 331 GtCO_2. The use of green hydrogen over the full period with 0% leakage rate would then results in a reduction of 331 GtCO_2 emitted into the atmosphere. The CO_2e emissions resulting from hydrogen leakage into the atmosphere and, in the case of grey and blue hydrogen, its production and transport, will reduce this avoided cumulative CO_2. Figure 4a shows that assuming a green hydrogen economy would result, assuming a 1% leakage rate and a 100-year time-horizon (GWP_100), in 327 GtCO_2e avoided. This abatement

decreases to 289 GtCO_2e for a 10% leakage rate. For a mix of blue + green hydrogen, 259 GtCO_2e are avoided for a 1% leakage rate at a 100 time-horizon (Fig. 4b). In 2030, a 33% fraction of grey hydrogen is still assumed in this scenario. When a of mix of grey + blue + green hydrogen is considered, according to the HC2017 scenario, the cumulative CO_2 emissions avoided total 258 GtCO_2e for a 1% leakage rate and using the GWP_100 metric (Fig. 4c). This abatement decreases to 103 GtCO_2e for a 10% leakage rate. The results show that in the case of blue and grey hydrogen, the climate benefit rapidly decreases when the leakage rate is >3%. A similar conclusion arises for the IEA2021 scenario (see "Methods" for a brief description of the IEA2021 scenario proposed by the International Energy Agency in 2021[53]) characterized by a higher contribution of blue hydrogen in 2050 compared to HC2021 (Supplementary Fig. S7a). Over the full 2030–2100 period, this scenario provides a cumulative CO_2 emission abatement of 353 GtCO_2. When the climate impact of the hydrogen leaks and production is considered, for a very low
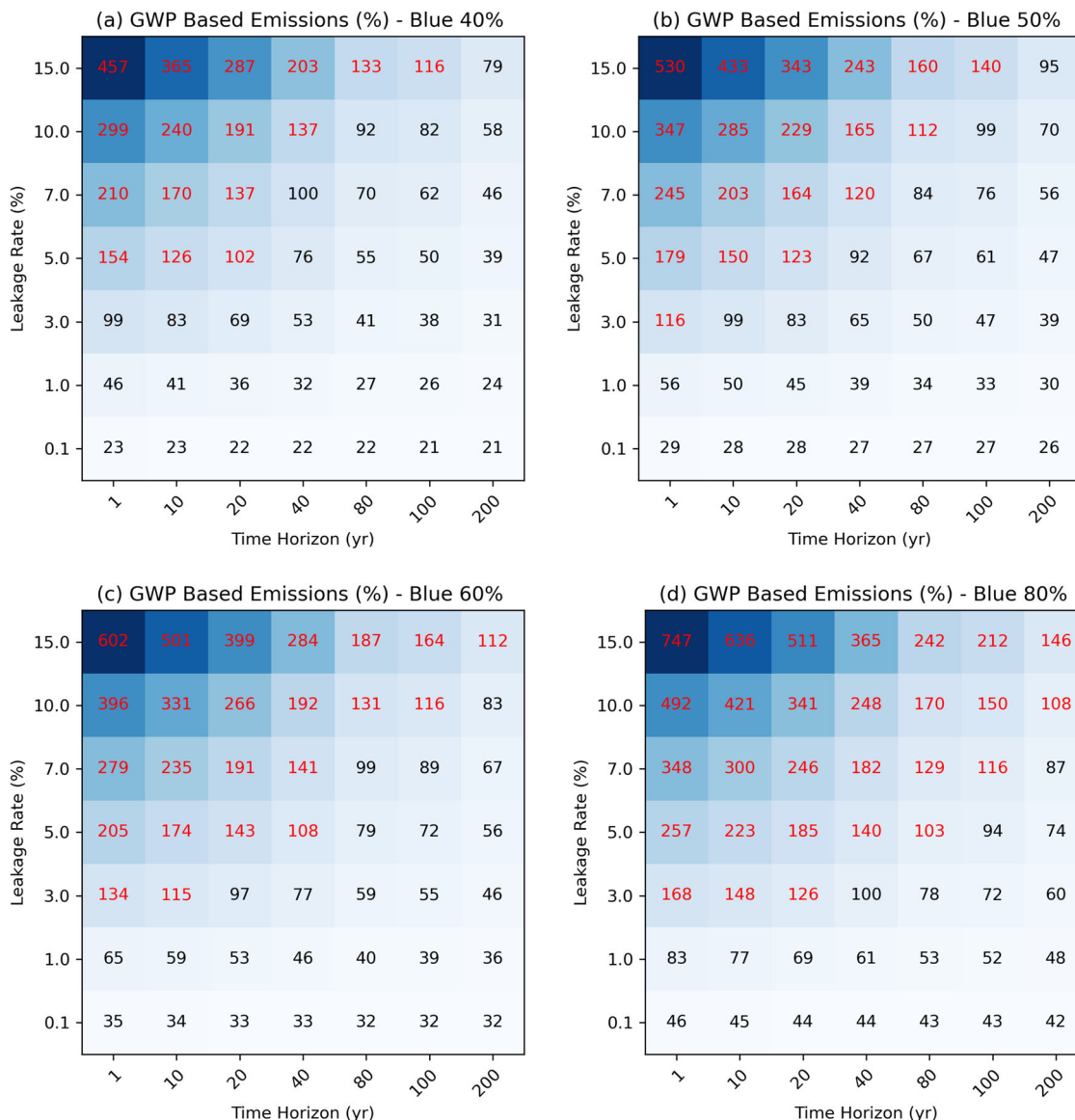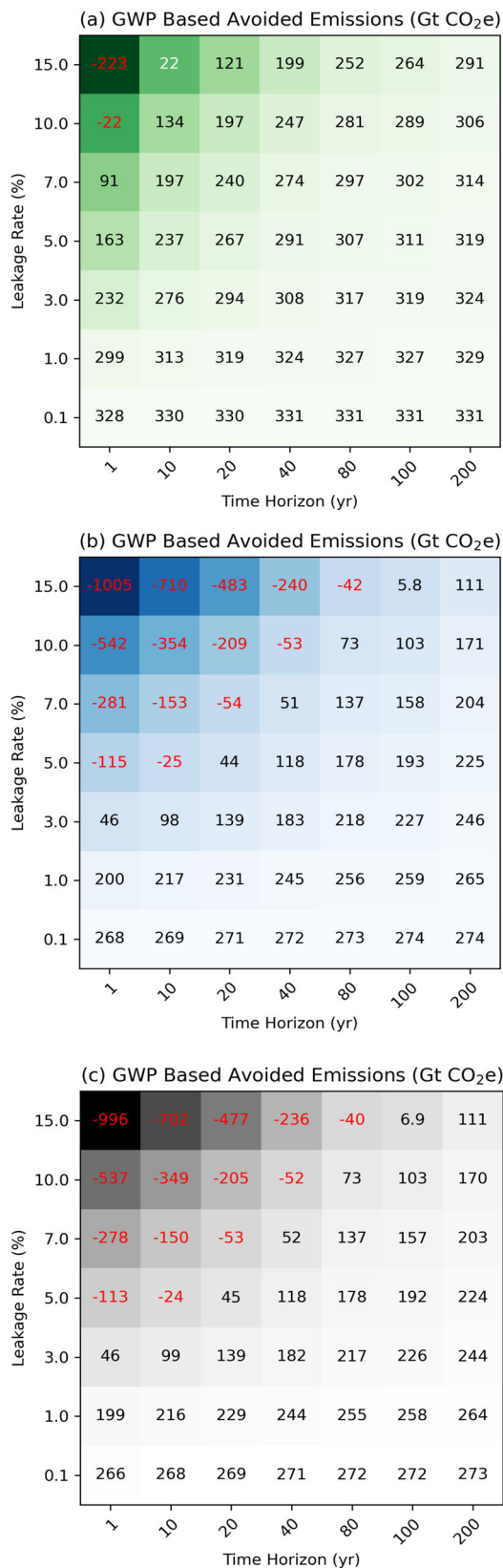
Fig. 3 Climate benefit of a global energy transition to hydrogen for various blue hydrogen mix. GWP based emission ratio (expressed in %) of CO_2 equivalent emissions associated with a hydrogen economy to the avoided CO_2 emissions as a function of the hydrogen leakage rate and the metric time-horizon. The emission ratios are calculated assuming a blue + green hydrogen with (**a**) 40%, (**b**) 50%, (**c**) 60%, and (**d**) 80% blue hydrogen supply. The net climate penalty conditions (ratios > 100%) are provided in red.

leakage rate of 0.1%, the CO_2 abatement is 270 $GtCO_2$e based on the GWP_{100} climate metric. For a leakage rate of 1%, we calculate an abatement of 252 $GtCO_2$e. This abatement is reduced to 60 $GtCO_2$e for a high leakage rate of 10%.

An alternative, more ambitious, roadmap for a transition to a hydrogen energy supply has also been considered. According to this HCMK2021 scenario (see "Methods" for a brief description of the HCMK2021 scenario proposed by the Hydrogen Council/ McKinsey & Company in 2021[54]), over the full 2030–2100 period, the resulting cumulative CO_2 emission abatement is 417 $GtCO_2$. When the climate impact of the hydrogen leaks and production is considered, the cumulative equivalent CO_2 emissions avoided is affected as depicted in Supplementary Fig. S7b. For a very low leakage rate of 0.1%, the CO_2 abatement is 395 $GtCO_2$e based on the GWP_{100} climate metric. For a leakage rate of 1%, we calculate an abatement of 388 $GtCO_2$e. This abatement is reduced to 310 $GtCO_2$e for a high leakage rate of 10%. This scenario, characterized by a decrease of grey and blue

hydrogen supply in order to reach 100% green hydrogen in 2050, clearly shows a larger climate benefit compared to HC2017 stressing the need for a rapid transition to a 100% green hydrogen economy.

Achieving an energy transition of the European Union (EU) compliant with the Paris Agreement and with the European ambitions for achieving climate neutrality by 2050 will require hydrogen deployement at large scale[55]. According to the TYNDP2022 scenario (see "Methods" for a brief description of the TYNDP2022 scenario proposed by ENTSOG and ENTSO-E in 2022[56]), 2496 TWh (9 EJ) are produced from hydrogen in 2050. Based on the energy content of gaseous hydrogen[3,7], this corresponds to a supply of 63 Mt H_2/year in 2050 with a 6% supply of blue hydrogen (3.8 Mt/year). The total energy production from hydrogen provides a total avoided CO_2 emissions of 620 Mt CO_2/year in 2050, or a total cumulative CO_2 abatement of 36.1 $GtCO_2$ over the full period 2030–2100. For this scenario related to European emissions, we use the

(a) GWP Based Avoided Emissions (Gt CO₂e)

(b) GWP Based Avoided Emissions (Gt CO₂e)

(c) GWP Based Avoided Emissions (Gt CO₂e)

Fig. 4 Abatement of cumulative CO_2 emissions associated with a global energy transition to hydrogen. CO_2 emissions abatement ($GtCO_2e$) over the 2030−2100 period associated with a worlwide hydrogen economy transition according to the HC2017 scenario and as a function of the leakage rate and GWP time-horizon. The hydrogen CO_2 equivalent emissions are calculated considering (**a**) green, (**b**) blue + green, and (**c**) grey + blue + green hydrogen according to the HC2017 scenario. The net climate penalty conditions (negative emissions) are provided in red.

the impact of hydrogen leaks is 35.7 $GtCO_2e$ for a 1% leakage rate and a 100 year time-horizon. This abatement decreases to 31.8 $GtCO_2e$ for a 10% leakage rate. For a mix of blue + green hydrogen (Fig. 5b), the abatement is reduced to 33.6 $GtCO_2e$ and 26.1 $GtCO_2e$ for a 1 and 10% leakage rate, respectively, based on the GWP_{100}. For a 20 year time-horizon metric, an abatement of 32.2 $GtCO_2e$ is calculated for a 1% leakage rate.

Discussion

The GWP_{100} is the reference metric for reporting emissions under UNFCCC to determine CO_2 equivalent emissions for a basket of greenhouse gases. Shorter time-horizons have also been suggested for SLCFs[4,36–38]. Reducing SLCFs can slow the projected global warming over the next 25 years with many synergies towards achieveving Sustainable Developments Goals (SDGs), in particular in terms of human and ecosystems health[37,57]. In the case of H_2, limited air quality or ecosystem impacts are however expected[21,58] and these synergies are probably minor. For methane fugitive emissions associated with grey and blue hydrogen production, the situation is different and a shorter time-horizon appears appropriate to account for synergies with air quality impacts. The time-horizon of the metric is therefore variable in our calculations in order to illustrate the sensitivity to the chosen metric and time-horizon. Based on our calculations, a clear benefit for climate arises from a transition to a green hydrogen economy. For a leakage rate of 1–3% and based on the GWP climate metric at 20–100 year time-horizon, the green hydrogen CO_2 equivalent emissions represent 1.2–11.3% of the CO_2 emissions avoided (0.2–5.0% based on the GTP). In the scenario considering a mix of blue (30%) and green (70%) hydrogen, we calculate for a leakage rate of 1–3%, a significantly lower climate benefit with hydrogen CO_2 equivalent emissions representing 20–54% of the abated CO_2 emissions based on the GWP_{20} and GWP_{100}. At leakage rates >10% (resp. 5%) and for a time-horizon of 100 year (resp. 20 year) the mix of green + blue hydrogen economy leads to a climate penalty with CO_2 equivalent emissions larger than the avoided CO_2 emissions. This moderate climate benefit (or even climate penalty) obtained in the case of a mix of blue + green hydrogen strongly decreases as the assumed blue hydrogen contribution to the energy portfolio increases.

Shorter time-horizons are less adequate for estimating the importance of a short-lived species such as H_2 for mitigating long-term climate change, as envisaged within the Paris Agreement[44,48,52]. The endpoint metric GTP appears as a more appropriate climate metric to estimate the effect of a short-lived climate forcer like H_2 on end of century climate goals and evaluate the mitigation potential within this framework. The CGTP metric combining sustained and pulse emission responses, also appears as a particularly appropriate instrument to convert emissions of the short-lived H_2 to equivalent cumulative carbon emissions[44]. The CGTP provides the cumulative emissions associated with a structural change such as the transition to a hydrogen energy supply. As a summary, and as an illustration of the use of CGTP to measure the mitigation progress towards a climate change objective at the end of the century, Fig. 6 shows

hydrogen metrics (i.e., GWP in Fig. 5 and CGTP in Fig. 6) calculated based on the hydrogen northern hemisphere lifetime (see Table 1). Figure 5 shows the cumulative CO_2 emissions abatement calculated based on the GWP as a function of the leakage rate and time-horizon. In the case of a green hydrogen supply (Fig. 5a), the cumulative CO_2 abatement accounting for
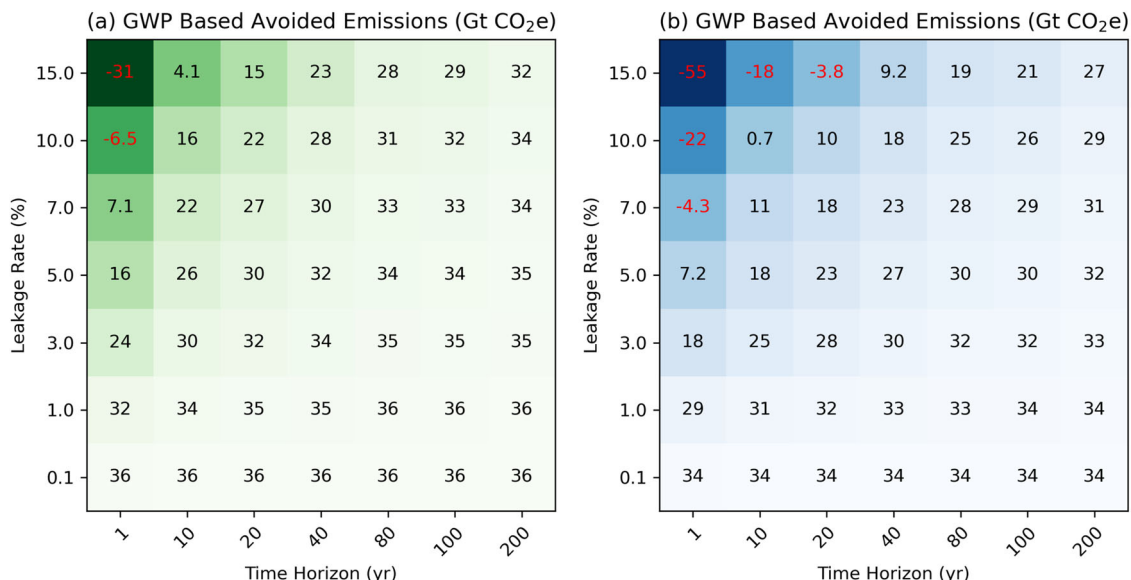
Fig. 5 Abatement of cumulative CO₂ emissions associated with an European energy transition to hydrogen. CO_2 emissions abatement (GtCO₂e) over the 2030–2100 period associated with an european hydrogen economy transition according to the TYNDP2022 scenario and as a function of leakage rate and GWP time-horizon. The hydrogen CO_2 equivalent emissions are calculated considering (**a**) green only, (**b**) blue + green hydrogen according to the TYNDP2022 scenario. The net climate penalty conditions (negative emissions) are provided in red.
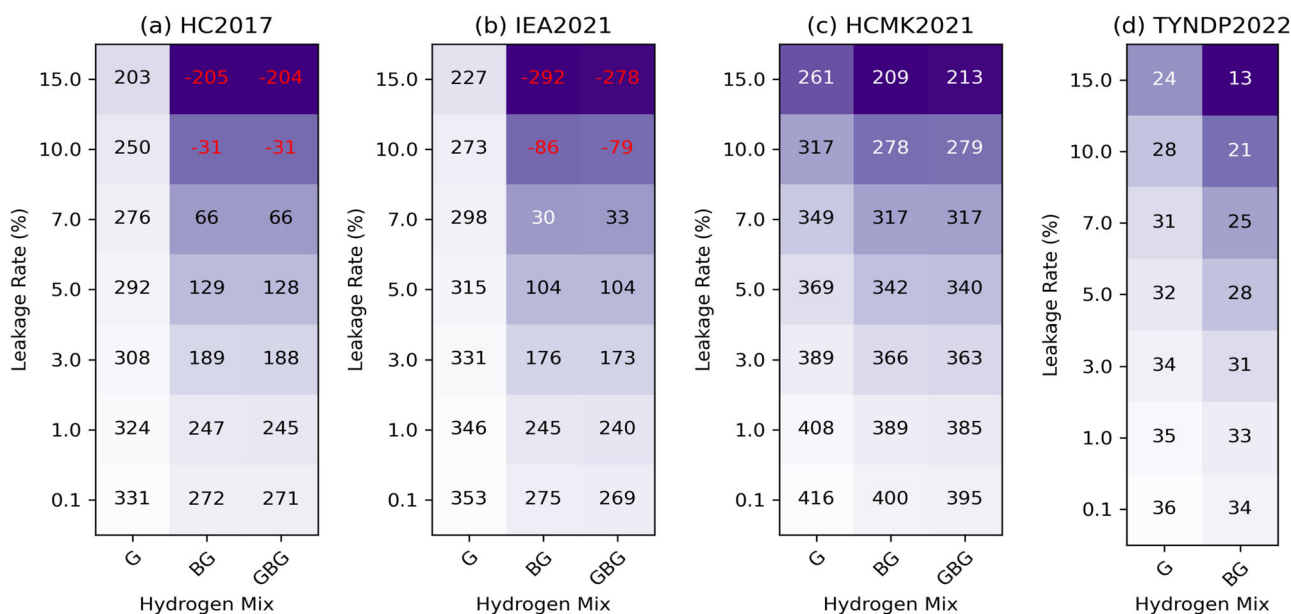
Fig. 6 Abatement of CO₂ emissions calculated based on the CGTP metric. Cumulative CO_2 equivalent emissions (GtCO₂e) abatement over the 2030–2100 period associated with a hydrogen economy as a function of hydrogen leakage rate. The CO_2 equivalent emissions are calculated based on the CGTP for four scenarios: (**a**) HC2017, (**b**) IEA2021, (**c**) HCMK2021, and (**d**) TYNDP2022. The emission abatement is calculated assuming three hydrogen portfolio: (G) green hydrogen supply only, (BG) a mix of blue + green hydrogen, and (GBG) a mix of grey + blue + green hydrogen. The net climate penalty conditions (negative emissions) are provided in red.

the cumulative carbon emissions saved by 2100 when the hydrogen economy is introduced for the different scenarios considered in this study over the 2030–2100 period. In the case of a green hydrogen economy, a cumulative worldwide CO_2 emission abatement of 324 GtCO₂e is calculated for a 1% leakage rate for the HC2017 scenario, 346 GtCO₂e for the IEA2021 scenario, and of 408 GtCO₂e for the more ambitious HCMK2021 scenario. A cumulative carbon emission abatement of 35 GtCO₂e is calculated for the TYNDP2022 European green hydrogen scenario. For a 10% leakage rate, under a green hydrogen economy assumption, the abatement is reduced to 250, 273, 317 and 28

GtCO₂e for the HC2017, IEA2021, HCMK2021, and TYNDP2022 scenarios, respectively. Interestingly, the comparison with Figs. 4a and 5a shows that these results are very close to the emission abatements calculated based on the GWP_{40}. This suggests, in agreement with previous work[59], that 40 years appears as an appropriate time-horizon to estimate the mitigation of CO_2 emissions due to a hydrogen economy and the resulting benefit on end of century climate. The cumulative CO_2 emission abatement is significantly reduced in the case of a mix blue + green hydrogen and decreases to 247 GtCO₂e for a 1% leakage rate for the HC2017 scenario considering 30% of blue hydrogen

after 2050. A climate penalty of -31 and -205 GtCO₂e is even calculated for higher leakage rates of 10 and 15%, respectively. For the IEA2021 scenario characterized by a higher blue hydrogen fraction, a climate penalty of -86 and -292 GtCO₂e is also calculated for leakage rates of 10 and 15%, respectively. The comparison with scenario HCMK2021 (0% blue hydrogen after 2050) providing CO₂ emissions abated by 389 and 278 GtCO₂e for 1 and 10% leakage rates, respectively, clearly shows the importance of a rapid replacement of the blue hydrogen supply by green hydrogen in order to preserve a clear climate benefit from a hydrogen economy.

All considered scenarios for a future hydrogen transition worldwide and in Europe, clearly show that a green hydrogen economy is beneficial in terms of mitigated CO₂ emissions for all policy-relevant time-horizons. In contrast, our results suggest that the CO₂ and CH₄ emissions associated with blue (and grey) hydrogen production and transport significantly reduce the benefit of a transition to a hydrogen economy and even introduce a climate penalty at high leakage rate or blue hydrogen market penetration. Reducing the leakage rate of H₂ (and of CH₄ in the case of blue hydrogen production) and increasing the green hydrogen production pathway appear as the key leverages towards a maximum mitigation of equivalent CO₂ emissions from a large-scale structural transition to a hydrogen economy.

It should be kept in mind, that the H₂ climate impact is indirect and is therefore subject to larger uncertainties than direct impacts from other climate pollutants. We estimate uncertainties on the H₂ metrics of about 40% on the GWP$_{100}$, 60% on the GTP$_{100}$ and 70% on the GTP$_{100}$. These typical uncertainties on the metrics directly translate into a similar uncertainty on the carbon equivalent emissions. Therefore, we stress the need for better constrained atmospheric models based on a reliable observational network in order to derive even more robust estimates of the hydrogen climate benefit.

Methods

Climate metrics calculations. We use analytical Impulse Response Functions (IRFs) to calculate the hydrogen GWP and GTP[52]. The mass of a species S evolves in time in the atmosphere according to:

$$\Delta M_S(t) = \int_{t_0}^{t} E_S(t') \mathrm{IRF}_S(t - t') \, dt' \tag{1}$$

where $M_S(t)$ is the species atmosphere mass (kg) at time t, $E_S(t)$ the emission of the species (kg/year), and t_0 is the initial year of integration (we assume $t_0 = 0$). The atmospheric mass M_S is converted to mixing ratio q_S (ppbv) with $q_S = 5.625 \times 10^{-9} M_S/m_S$, where m_S is the molecular mass.

The H₂ IRF is a simple exponential decay function with a characteristic atmospheric global lifetime τ_{H_2} of 2.5 years (corresponding to a global tropospheric lifetime of 2.1 years)[15]:

$$\mathrm{IRF}_{H_2}(x) = \exp\left(-\frac{x}{\tau_{H_2}}\right) \tag{2}$$

A similar IRF is used for methane with a perturbation lifetime τ_{CH_4} of 12.4 years[43]. The IRF for CO₂ is calculated with refs. 52, 60:

$$\mathrm{IRF}_{CO_2}(x) = a_0 + \sum_{i=1}^{3} a_i \exp\left(-\frac{x}{b_i}\right) \tag{3}$$

with $a_0 = 0.217$, $a_1 = 0.259$, $a_2 = 0.338$, $a_3 = 0.186$, $b_1 = 172.9$ year, $b_2 = 18.51$ year, and $b_3 = 1.186$ year. These parameters used in the IRF were determined from a 400 GtC impulse emission in the Bern carbon cycle model[52,60].

The CO₂ radiative forcing (RF, or ERF) is then calculated based on the calculated $\Delta q_{CO2}(t)$ and the radiative forcing efficiency[41] of 1.33×10^{-5} W m^{-2} ppbv^{-1}. For H₂ indirect forcings, a similar procedure is used based on the GFDL-AM4.1 radiative forcings efficiencies[15]. The H₂ forcing is further decomposed into its various components corresponding to the stratospheric H₂O, tropospheric and stratospheric ozone components and for these forcings the H₂ lifetime is used.

A special treatment is used for the methane perturbation associated with the change in OH resulting from H₂ emissions in order to account for the different lifetime of the perturbation. The methane lifetime associated with OH oxidation 9.7 years in the GFDL-AM4 model[40] is adjusted to account for the stratospheric loss of methane with a lifetime of 120 years, and for the methane soil uptake with a

lifetime of 160 years. Based on the change in OH of +8% for a 200 Tg H₂ emission increase[15], the steady state methane concentration due to the H₂ perturbation is calculated with[61,62]:

$$\Delta q_{CH4}^{SS} = f \, q_{CH4}^{ref} \Delta\tau_{CH4} \tag{4}$$

where Δq_{CH4}^{SS} is the steady-state change in methane mixing ratio due to H₂ increase in the atmosphere per TgH₂, q_{CH4}^{ref} (1808 ppbv) is the reference methane mixing ratio, $f = 1.3$[15] denotes the methane feedback on its own lifetime and $\Delta\tau_{CH4}$ (%/TgH₂) is the change in methane lifetime per TgH₂. We approximate the change in methane due to the H₂ impact on OH with[63]:

$$\Delta M_{CH4}(t) = \Delta q_{CH4}^{SS} \int_{t_0}^{t} \Delta M_{H2}(t') \left[(1 - e^{-\frac{1}{\tau_{CH4}}}) \delta(t' - t_0) \right. $$
$$\left. + (1 - e^{-\frac{1}{\tau_{CH4}}}) e^{\frac{(t - t')}{\tau_{CH4}}} (1 - \delta(t' - t_0)) \right] dt' \tag{5}$$

where $\delta(x)$ is the Dirac function. Each year following the hydrogen pulse emission, due to the change in H₂, CH₄ increases towards the steady-state perturbation (first term of equation) and decreases exponentially from this value the following years (second term). Supplementary Fig. S8a shows the response of the atmospheric mass of H₂, CH₄, and CO₂ after a pulse emission of H₂ (and CO₂) of 1 Tg. H₂ decreases exponentially after emission with a characteristic lifetime τ_{H_2} and CO₂ decreases with a much longer lifetime τ_{CO_2}. Methane resulting from the H₂ increase in the atmosphere and the subsequent perturbation in OH, increases from 0 to a peak of 60 pptv 4 years after the initial 1 TgH₂ emission. This value is in agreement with the 80 pptv calculated with the STOCHEM three-dimensional model[28] for 1.67 TgH₂ (i.e. 48 pptv/TgH₂). The peak CH₄ increase is however larger in our estimate, essentially due a shorter H₂ tropospheric lifetime in STOCHEM (1.6 year) compared to GFDL-AM4.1 (2.1 year). Based on the calculated change in methane mixing ratio, the radiative forcing efficiency of 44.3×10^{-5} W m^{-2} ppbv^{-1} is used[45] to derive the associated radiative forcing. The direct methane forcing is increased to account for the indirect tropospheric ozone (0.116×10^{-3} W m^{-2} ppbv^{-1}) and stratospheric H₂O (0.027×10^{-3} W m^{-2} ppbv^{-1}) forcings[64]. The indirect CO₂ produced from CH₄ oxidation[64,65] is not accounted for in this work. The tropospheric ozone and stratospheric water vapour forcings reported with GFDL-AM4.1 are associated with both H₂ and CH₄ changes. In our calculations, the methane forcing also accounts for the indirect tropospheric O₃ and stratospheric H₂O indirect contributions. In order to avoid double counting, we calculate the methane forcing at steady-state for a 1 Tg H₂ perturbation. This forcing is higher that the methane forcing calculated with GFDL-AM4.1 due to these indirect ozone and stratropheric H₂O contributions included. The tropospheric ozone and stratospheric H₂O radiative forcing efficiencies from GFDL-AM4.1 are then rescaled in order to account for this difference and hence separate the H₂ and CH₄ impact on these forcings.

The climate response, in terms of global surface temperature change, is also estimated based on an IRF[52]:

$$\Delta T(t) = \int_{t_0}^{t} RF(t') \, \mathrm{IRF}_T(t - t') \, dt' \tag{6}$$

The climate response IRF$_T$ is provided by:

$$\mathrm{IRF}_T(x) = \frac{1}{\lambda} \sum_{i=\{s,f\}} \frac{c_i}{d_i} \exp\left(-\frac{x}{d_i}\right) \tag{7}$$

where λ is the climate sensitivity parameter, and subscripts f and s refer to the fast and slow climate responses, respectively. The updated coefficients[66,67] of IRF$_T$ are: $c_f = 0.587$, $c_s = 0.413$, $d_f = 4.1$ year, and $d_s = 249$ year. The sum of the c_s and c_f coefficients is normalized and the climate sensitivity parameter, $\lambda = 1.04$ W/m²/K, is introduced in the IRF, assuming a 3.78 K warming for a CO₂ doubling radiative forcing (3.93 Wm^{-2})[41]. Supplementary Fig. S8b, c show the resulting radiative forcing and temperature change after a 1Tg pulse emission of H₂ (or CO₂). The additional carbon cycle responses to temperature are excluded in our calculations[68].

The Absolute GWP (AGWP) of H₂ is calculated based on:

$$\mathrm{AGWP}_{H_2}(t_h) = \int_{t_0}^{t_h} RF_{H_2}(t) \, dt \tag{8}$$

The GWP of H₂ is then calculated by definition as the ratio between the AGWP of H₂ (or individual components) relative to the AGWP for CO₂:

$$\mathrm{GWP}_{H2}(t_h) = \frac{\mathrm{AGWP}_{H2}(t_h)}{\mathrm{AGWP}_{CO2}(t_h)} \tag{9}$$

This methodology is repeated in order to decompose GWP$_{H2}$ into its various individual components (i.e., GWP$_{CH4}$, GWP$_{H2O}$, GWP$_{O3t}$, GWP$_{O3s}$), substituting RF$_{H_2}$ by the individual radiative forcings of methane, stratospheric water vapour, tropospheric ozone, and stratospheric ozone.

The Absolute GTP (AGTP) of H_2 is calculated based on:

$$\text{AGTP}_{H_2}(t_h) = \int_{t_0}^{t_h} \text{RF}_{H_2}(t)\,\text{IRF}_T(t_h - t)\,dt = \Delta T_{H_2}(t_h) \quad (10)$$

The GTP is calculated by definition as the ratio between the AGTP of H_2 (or of its individual components) and the AGTP for CO_2:

$$\text{GTP}_{H2}(t_h) = \frac{\text{AGTP}_{H2}(t_h)}{\text{AGTP}_{CO2}(t_h)} \quad (11)$$

The emission profile $E_{H_2}(t)$ (or E_{CO_2}) is taken to be a pulse emission of 1 Tg for the calculation of the pulse metrics GWP_p and GTP_p or a step sustained emission of 1 Tg for the sustained metrics GWP_s and GTP_s. It should be noted, that the exact definition of the GWP refers to an instantaneous pulse emission. In our calculations, a time-step of 1 year is considered, implying a 1-year pulse emission even for GWP_p. This limitation induces a 10% difference in the $\text{GWP}_{p,100}$ calculation[3].

In order to derive the combined metrics[44], we first define the Absolute Global Forcing Potential (GFP):

$$\text{AGFP}_{H_2}(t_h) = \int_{t_0}^{t_h} \text{RF}_{H_2}(t_h - t)\delta(t - t_0)\,dt = \text{RF}_{H_2}(t_h) \quad (12)$$

Similar to the AGTP which provides the temperature at a considered time-horizon, the AGFP is an end-point metric providing the radiative forcing at a considered time-horizon. The H_2 Combined GWP (CGWP) is then calculated with:

$$\text{CGWP}_{H2}(t_h) = \frac{\text{AGFP}_{H2,s}(t_h)}{\text{AGFP}_{CO2}(t_h)} \quad (13)$$

and the H_2 Combined GTP (CGTP) is calculated with:

$$\text{CGTP}_{H2}(t_h) = \frac{\text{AGTP}_{H2,s}(t_h)}{\text{AGTP}_{CO2}(t_h)} \quad (14)$$

where the subscript 's' refers to the sustained emission metrics.

The uncertainties in the H_2 and CH_4 metrics are estimated following the exact same methodology as developed and presented by IPCC[41]. Since a large fraction of the H_2 indirect climate impact is associated with methane, several uncertainties are similar for these two species. Supplementary Tables S1 and S2 provide, for respectively CH_4 and H_2, the total uncertainty calculated in various metrics, as a percentage of the best estimate and expressed as 90% confidence interval. The uncertainties are also provided by component of the total emission metric calculation (radiative efficiency, chemical response and feedbacks, atmospheric lifetime, CO_2 combined uncertainty in radiative efficiency and CO_2 impulse response function, carbon cycle response, fate of oxidized fossil methane, and impulse-response function for temperature increase). The uncertainties in individual terms are taken from Section 7.6 of IPCC AR6 report[41], except for the CO_2 impulse response which comes from Joos and Bruno[60]. The uncertainties are however modified for H_2 when needed, in particular the lifetime uncertainty is estimated assuming a H_2 atmospheric lifetime uncertainty of 0.5 year around our best estimate of 2.5 year. The uncertainties on the temperature impulse-response function were recalculated by taking 1.645 x standard deviation of the GTPs generated from 600 ensemble members of the impulse response derived from two climate emulators (see Forster et al.[41] for more details). The resulting estimated total uncertainty in the H_2 GWP is 31–36%. A value in agreement with previous estimates[35]. The uncertainty on the H_2 GTP ranges from 131 to 64% and is largely dominated by the climate response function uncertainty. The uncertainty on the GTP is in the range 47–73%. These uncertainties on the metrics directly translate into similar uncertainties on the calculated CO_2 equivalent emissions.

Future hydrogen emission scenarios. The estimated hydrogen production in 2020 is 87[53]–90[54] Mt H_2/year. It is beyond the scope of this study to propose future hydrogen energy supply scenarios. Instead, we base our analysis on the scenarios developed by the Hydrogen Council for the worldwide hydrogen energy transition and on the European Union (EU) roadmap for a future hydrogen economy in Europe. These scenarios are succinctly summarized below and we refer the reader to the full reports for a more in-depth overview of the underlying economic and energy assumptions. The worldwide energy transition scenario used in this study is based on the scenario developed by the Hydrogen Council as a roadmap for long-term hydrogen deployment[50]. This scenario (referred to as HC2017) analyses the possible deployment of hydrogen in the various sectors: transportation, industrial energy, building heating and power, industry feedstock and power generation, and assumes an almost eight-fold increase in hydrogen demand between 2020 and 2050. According to this scenario the global energy supply of hydrogen was 10 EJ (2778 TWh) in 2020, and is projected to increase to 14 EJ (3889 TWh) in 2030; 28 EJ (7778 TWh) in 2040, and 78 EJ (21,667 TWh) in 2050. In this study, we use a hydrogen energy density of 142 MJ/kg as used in previous work[3,4,11,50]. This value is the Higher Heating Value (HHV) of the hydrogen fuel defined as the amount of heat released once it is combusted and the products have returned to a temperature

of 25 °C, considering the latent heat of vaporization of water in the combustion products. Currently, the hydrogen technologies do not condense the water to use the full heating value of hydrogen. The hydrogen Lower Heating Value (LHV) of 120 MJ/kg, defined as the amount of heat released by combusting hydrogen and returning the temperature of the combustion products to 150 °C, and hence assuming that the latent heat of vaporization of water in the reaction products is not recovered, should be used. For consistency with previous work but also assuming an improvement of the hydrogen technologies over the next 30 years, we apply the HHV in our analysis. Based on this value we derive a production of 98 Mt H_2/year in 2030, 197 Mt H_2/year in 2040 and 549 Mt H_2/year in 2050. Using the LHV instead of the HHV would increase the hydrogen production for a given energy demand by 18% and provide 650 Mt H_2/year in 2050. The sensitivity of the results to the use of the LHV instead of the HHV will be illustrated. Please note that using the LHV (more consistent with current hydrogen technologies), we derive a hydrogen production in 2020 (estimated in 2017[50]) of 83 Mt H_2/year, a value lower by 4–8% compared to the actual production reported for 2020[53,54]. In addition to this total energy supply, this scenario further assumes a phase-out of grey hydrogen by 2040 and an increased supply of blue and green hydrogen to about 33% grey, 33% blue, and 33% green in 2030; 50% blue in 2030, and 30% blue in 2050[51]. For the year 2050, the HC2017 scenario results in an annual 6 GtCO_2/year abatement. We assume the 2050 values over the period 2050–2100. Over the entire 2030–2100 period, the HC2017 scenario results in a cumulative CO_2 emission abatement of 331 GtCO_2.

There is a continued acceleration in hydrogen deployment and a strong momentum for future transition to an hydrogen economy. A more ambitious hydrogen scenario with hydrogen reaching 22% of the global energy demand in 2050 has been developed by the Hydrogen Council and McKinsey & Company[54]. According to this scenario (referred to as HCMK2021), the hydrogen worldwide end-use demand increases from 20 EJ (5555 TWh) in 2030; 55 EJ (15,278 TWh) in 2040; to 94 EJ (26,111 TWh) in 2050. This corresponds to 140, 385, and 660 Mt H_2/year in 2030, 2040 and 2050, respectively. This scenario further assumes 50%, 30 and 20% of grey, blue, and green hydrogen, respectively, in 2030; 5% 40%, and 55%, respectively in 2040; and 100% green hydrogen in 2050. The HCMK2021 scenario results in an annual CO_2 emission abatement of 7 GtCO_2/year in 2050. If we further assume the 2050 values constant for the following decades, over the entire 2030–2100 period, the HCMK2021 scenario results in a cumulative CO_2 emission abatement of 417 GtCO_2. Other scenarios for future hydrogen production have been developed. In particular, in its "Net Zero by 2050" roadmap, the International Energy Agency (referred to as IEA2021) assumes a future hydrogen supply of 212 Mt H_2/year in 2030, 390 Mt H_2/year in 2040, and 528 Mt H_2/year in 2050[53]. This scenario further assumes 30%, 32 and 38% of grey, blue, and green hydrogen, respectively, in 2030, and 9%, 38%, and 53%, respectively in 2040. In 2050, this scenario still assumes a significant fraction of blue hydrogen with 1% of grey, 37% of blue, and 62% of green hydrogen. The IEA2021 scenario results in an annual CO_2 emission abatement of 5.7 GtCO_2/year in 2050. If we further assume the 2050 values constant for the following decades, over the entire 2030–2100 period, the IEA2021 scenario results in a cumulative CO_2 emission abatement of 353 GtCO_2. Another set of three future scenarios for global scale transition to an hydrogen economy has also been proposed by Bloomberg NEF[69]. These scenarios estimate a total energy demand for hydrogen in 2050 of 27 EJ (190 Mt H_2/year), 99 EJ (697 Mt H_2/year), and 195 EJ (1373 Mt H_2/year) for the "Weak Policy", "Strong Policy" and "Theoretical Max" scenarios, respectively. We note that the "Strong Policy" scenario is close to the HCMK2021 scenario. In addition, the "Theoretical Max" scenario, which assumes that all unlikely-to-electrify sectors in the economy use hydrogen, suggests that there is an enormous potential for hydrogen use in the economy, resulting in a yearly CO_2 abatement of almost 15 GtCO_2/year in 2050. In this study we focus on the HC2017 and further illustrate the HCMK2021 and IEA2021 scenarios which cover a reasonable range allowing to assess the sensitivity of the results to the development of a future hydrogen economy, but we note that other scenarios are also available.

The European Union (EU) has issued an hydrogen roadmap aiming at generating 8.1 EJ (2250 TWh) of hydrogen in 2050, representing roughly a quarter of the EU's total energy demand[53]. Achieving this objective would reduce EU annual CO_2 emissions by about 560 Mt CO_2 in 2050. Instead of using this scenario, we rather use a more recent and slightly more ambitious scenario developed for European future energy transition by the European Network of Transmission System Operators for Gas and Electricity (ENTSOG/ENTSO-E)[55]. The "Global Ambition" scenario[55] (referred to here as TYNDP2022) pictures a EU pathway to achieving carbon neutrality by 2050 with a hydrogen demand developing as of 2030 and becoming the main gas energy carrier in 2050. According to this scenario 1.7 EJ (466 TWh) are produced from hydrogen in 2030; 5.7 EJ (1575 TWh) in 2040; and 9.0 EJ (2496 TWh) in 2050; corresponding to a supply of 12 Mt H_2/year in 2030, 40 Mt H_2/year in 2040 and 63 Mt H_2/year in 2050. The TYNDP2022 scenario further assumes a phase-out grey hydrogen before 2030, and 51%, 13.5 and 6% of blue hydrogen in 2030, 2040, and 2050, respectively. This scenario reduces the annual CO_2 emissions by 620 MtCO_2/year in 2050. Assuming 2050 values for the following decades, the TYNDP2022 scenario leads to a mitigation of cumulative CO_2 emissions of 36 GtCO_2 over the full period 2030–2100.

Carbon dioxide and methane emissions from blue and grey hydrogen. At present, 95% of the hydrogen is produced via the Steam Methane Reforming (SMR) process using fossil natural gas as a feedstock[70]. The CO_2 emissions from grey hydrogen production were recently calculated[4] considering both the CO_2 emissions during the SMR process itself (38.5 gCO_2/MJ), during the heat and electricity generation needed to drive the SMR process (31.8 gCO_2/MJ), and the upstream emission from the energy used to produce, process and transport natural gas and hydrogen (5.3 gCO_2/MJ). The sum of these three terms (75.6 gCO_2/MJ), combined with the energy content of gaseous hydrogen (7 gH_2/MJ) provides an emission of 10.8 kgCO_2/kgH_2. We also account for the methane needed to produce hydrogen[4]. The methane needed for the SMR process itself (14.04 gCH_4/MJ) plus the amount burned to generate the heat and pressure needed for SMR (11.6 gCH4/MJ) provides a total of 25.6 gCH4/MJ, or 3.65 kgCH_4/kgH_2. Based on this total methane amount, we account for the leakage during production and use of unburned methane to the atmosphere with a leakage fraction fl_{CH4} (see below). The total methane amount needed is slighly larger than the previous estimates of 3.0 kgCH_4/kgH_2[71] and 3.2 kgCH_4/kgH_2[5].

Blue hydrogen differs from grey hydrogen because some of the carbon dioxide released by the SMR process or/and heat and pressure generation is captured. We use capture rates[4] of 85% efficiency for SMR and 65% efficiency for driving the SMR. The total CO_2 emissions remaining, assuming CO_2 capture for both processes, is therefore 15% × 38.5 gCO_2/MJ + 35% × 31.8 gCO_2/MJ = 16.9 gCO_2/MJ. In addition, we consider the energy required to capture carbon dioxide[4]. The CO_2 emissions associated with carbon sequestration during both SMR and energy production to drive SMR is 16.3 gCO_2/MJ[4]. An additional emission of 6.5 gCO_2/MJ is added for indirect upstream emissions, providing a total CO_2 emission from blue hydrogen production and transport of 39.7 gCO_2/MJ, or 5.7 kgCO_2/kgH_2. This value, which accounts in particular for the energy needed to ensure the carbon sequestration, is significantly higher than previous estimate[51] of 1.5 kgCO_2/kgH_2. The methane amount needed for blue hydrogen is similar to grey hydrogen except for the amount associated with the increased energy needed to drive the carbon sequestration process[4]. This amount is estimated at 6.0 gCH_4/MJ, providing a total ammout of CH_4 of 31.6 gCH_4/MJ, or 4.5 kgCH_4/kgH_2. Based on this total methane amount, we apply a leakage fraction fl_{CH4} (see below) to account for unburned methane emission to the atmosphere. The equivalent CO_2 emissions, at a given time-horizon, from methane leakage during the grey and blue hydrogen production are calculated by multiplying the methane fugitive emissions by the corresponding recalculated methane climate metric (see Supplementary Table S3).

The hydrogen leakage rate fl_{H2} is varied in our calculations from 0.1 to 15% in order to calculate the hydrogen climate footprint. The overall methane leakage rate fl_{CH4} was recently estimated at 3.5%[4]. In this study, we derive fl_{CH4} based on the considered fl_{H2}. Due to its lower volumetric density compared to natural gas, it is estimated that H_2 will be transported at three times the pressure of natural gas[5]. At these higher pressures and since the gas viscosity of H_2 is lower than CH_4, the leakage rate of H_2 is calculated 3.7–4.5 times higher than CH_4 (assuming that most of the flow is laminar). Based on these values, we assume a volumetric leakage ratio between fl_{H2} and fl_{CH4} of 4. For emissions, we are interested by the mass of leakage and this ratio needs to be divided by the density ratio of CH_4 to H_2 (0.72 kg m^{-3}/0.09 kg m^{-3} = 8), providing fl_{H2} / fl_{CH4} = 0.5[5]. The methane fugitive emission needs to be corrected in order to account for the fact that hydrogen is deployed in order to replace natural gas use[29]. A fraction of the CH_4 fugitive emissions would hence also be released to the atmosphere under the use of fossil fuel natural gas use. We have assumed a methane amount of 25.6 gCH_4/MJ needed for hydrogen production[4]. For methane (natural gas), we assume an energy content of 53.6 MJ/kg[72] or 18.6 gCH_4/MJ. The difference (25.6–18.6) 7.0 gCH_4/MJ is the additional methane amount needed for hydrogen production. The calculated fugitive methane emission is hence corrected and multiplied by a 0.27 ratio (7.0/25.6). In the case of blue hydrogen, accounting for the additional methane needed for carbon sequestration provides a difference between hydrogen production and natural gas use of (31.6–18.6) 13.0 gCH_4/MJ, and a correction factor of 0.41 (13.0/31.6). The methane leakage rate fl_{CH4} is then equal to 0.54 fl_{H2} in the case of grey hydrogen and 0.82 fl_{H2} for blue hydrogen.

Data availability
The GFDL-AM4.1 model results used in this study are available at https://drive.google.com/drive/u/1/folders/1JNDcA8tdaVfHNmr1OuZzJnFPX7uqOZ-N. The H_2 and CH_4 climate metrics calculated in this study as a function of the time horizon are available at https://doi.org/10.5281/zenodo.7244779.

Code availability
The Fortran programs used to calculate the H_2 and CH_4 climate metrics and the Python codes used for analyzing the data and plotting are available at https://doi.org/10.5281/zenodo.7244779.

References
1. United Nations Framework Convention on Climate Change. *Adoption of the Paris Agreement, 21st Conference of the Parties, Paris, United Nations.* https://unfccc.int/resource/docs/2015/cop21/eng/l09r01.pdf (2015).
2. Van Ruijven, B., Lamarque, J.-F., van Vuuren, D. P., Kram, T. & Eerens, H. Emission scenarios for a global hydrogen economy and the consequences for global air pollution. *Glob. Environ. Change* **21**, 983–994 (2011).
3. Field, R. A. & Derwent, R. G. Global warming consequences of replacing natural gas with hydrogen in the domestic energy sectors of future low-carbon economies in the United Kingdom and the United States of America. *Int. J. Hydrogen Energy* **46**, 30190–30203 (2021).
4. Howarth, R. W. & Jacobson, M. Z. How green is blue hydrogen? *Energy Sci. Eng.* **9**, 1676–1687 (2021).
5. Cooper, J., Dubey, L., Bakkaloglu, S. & Hawkes, A. Hydrogen emissions from the hydrogen value chain-emissions profile and impact to global warming. *Sci. Total. Environ.* **830**, 154624 (2022).
6. Bond, S. W., Gül, T., Reimann, S., Buchmann, B. & Wokaun, A. Emissions of anthropogenic hydrogen to the atmosphere during the potential transition to an increasingly H_2-intensive economy. *Int. J. Hydrogen Energ.* **36**, 1122–1135 (2011).
7. Suleman, F., Dincer, I. & Agelin-Chaab, M. Environmental impact assessment and comparison of some hydrogen production options. *Int. J. Hydrogen Energy* **40**, 6976–6987 (2015).
8. Kammen, D. M. & Lipman, T. E. Assessing the future hydrogen economy. *Science* **302**, 226–229 (2003).
9. Roueff, E. et al. The full infrared spectrum of molecular hydrogen. *Astron. Astrophys.* **630**, A58 (2019).
10. Derwent, R. G., Collins, W. J. & Johnson, C. E. Stevenson Transient behaviour of tropospheric ozone precursors in a global 3-D CTM and their indirect greenhouse effects. *Clim. Change* **49**, 463–487 (2001).
11. Derwent, R. G. et al. Global environmental impacts of the hydrogen economy. *Int. J. Nuclear Hydrogen Product. Appl.* **1**, 57–67 (2006).
12. Ehhalt, D. H. & Rohrer, F. The tropospheric cycle of H_2: a critical review. *Tellus (B)* **61**, 500–535 (2009).
13. Derwent, R. G. *Hydrogen for Heating: Atmospheric Impacts, A Literature Review.* (Department of Business, Energy, and Industrial Strategy, United Kingdom, 2018).
14. Patterson, J. D. et al. Atmospheric history of H2 over the past century reconstructed from South Pole firn air. *Geophys. Res. Lett.* **47**, e2020GL087787 (2020).
15. Paulot, F. et al. Global modeling of hydrogen using GFDL-AM4.A: Sensitivity of soil removal and radiative forcing. *Int. J. Hydrogen Energ.* **46**, 13446–13460 (2021).
16. Hauglustaine, D. & Ehhalt, D. A three-dimensional model of molecular hydrogen in the troposphere. *J. Geophys. Res.* **107**, 4330–4346 (2002).
17. Sanderson, M. G., Collins, W. J., Derwent, R. G. & Johnson, C. E. Simulation of global hydrogen levels using a Lagrangian three-dimensional model. *J. Atmos. Chem.* **46**, 15–28 (2003).
18. Bousquet, P. et al. A three-dimensional synthesis inversion of the molecular hydrogen cycle: Sources and sinks budget and implications for the soil uptake flux. *J. Geophys. Res.* **116**, D01302 (2011).
19. Morfopoulos, C. et al. A global model for uptake of atmospheric hydrogen by soils. *Global Biogeochem. Cycles* **26**, GB3013 (2012).
20. Novelli, P. C. et al. Molecular hydrogen in the troposphere: Global distribution and budget. *J. Geophys. Res.* **104**, 30,427–30,444 (1999).
21. Schultz, M. G., Diehl, T., Brasseur, G. P. & Zittel, W. Air pollution and climate-forcing impacts of a global hydrogen economy. *Science* **302**, 624–627 (2003).
22. Prather, M. J. An environmental experiment with H_2? *Science* **302**, 581–582 (2003).
23. Jacobson, M. Z., Colella, W. G. & Golden, D. M. Cleaning the air and improving health with hydrogen fuel-cell vehicles. *Science* **308**, 1901–1905 (2005).
24. Warwick, N. J., Bekki, S., Nisbet, E. G. & Pyle, J. A. Impact of a hydrogen economy on the stratosphere and troposphere studied in a 2-D model. *Geophys. Res. Lett.* **31**, L05107 (2004).
25. Vogel, B., Feck, T., Grooß, J. U. & Riese, M. Impact of a possible future global hydrogen economy on Arctic stratospheric ozone loss. *Energy Environ. Sci.* **5**, 6445–6645 (2012).
26. Feck, T., Grooß, J.-U. & Riese, M. Sensitivity of Arctic ozone loss to stratospheric H_2O. *Geophys. Res.Lett.* **35**, L01803 (2008).
27. Tromp, T. K., Shia, R.-L., Allen, M., Eiler, J. M. & Yung, Y. L. Potential environmental impact of a hydrogen economy on the stratosphere. *Science* **300**, 1740–1742 (2003).

28. Derwent, R. G. et al. Global modelling studies of hydrogen and its isotopomers using STOCHEM-CRI: likely radiative forcing consequences of a future hydrogen economy. *Int. J. Hydrogen Energy* **45**, 9211–9221 (2020).

29. Ocko, I. B. & Hamburg, S. P. Climate consequences of hydrogen emissions. *Atmos. Chem. Phys.* **22**, 9349–9368 (2022).

30. Van Renssen, S. The hydrogen solution? *Nature Clim. Change* **10**, 799–801 (2020).

31. Alvarez, R. A. et al. Greater focus needed on methane leakage from natural gas infrastructure. *Proc. Natl. Acad. Sci. USA* **109**, 6435–6440 (2012).

32. Alvarez, R. A. et al. Assessment of methane emissions from the U.S. oil and gas supply chain. *Science* **361**, 186–188 (2018).

33. Defratyka, S. M. et al. Mapping urban methane sources in Paris, France. *Environ. Sci. Technol.* **55**, 8583–8591 (2021).

34. Pearman, G. I., Prather, M. J., Derwent, R. G., Don't rush into a hydrogen economy until we know all the risks to our climate. *Conversation. Australia.* https://theconversation.com/dont-rush-into-a-hydrogen-economy-until-we-know-all-the-risks-to-our-climate−140433 (2020).

35. Warwick, N. et al. *Atmospheric Implications of Increased Hydrogen Use.* (Department of Business, Energy, and Industrial Strategy, United Kingdom, 2022).

36. Ocko, I. B. et al. Unmask temporal trade-offs in climate policy debates. *Science* **356**, 492–293 (2017).

37. Shindell, D. et al. A climate policy pathway for near- and long-term benefits. *Science* **356**, 493–494 (2017).

38. Fesenfeld, L. K., Schmidt, T. S. & Schrode, A. Climate policy for short- and long-lived pollutants. *Nature Clim. Change* **8**, 924–936 (2018).

39. Lynch, J., Cain, M., Pierrehumbert, R. & Allen, M. Demonstrating GWP*: a means of reporting warming-equivalent emissions that captures the contrasting impacts of short- and long-lived climate pollutants. *Environ. Res. Lett.* **15**, 044023 (2020).

40. Horowitz, L. H. et al. The GFDL global atmospheric chemistry-climate model AM4.1: Model description and simulation characteristics. *J. Adv. Model. Earth Syst.* **12**, e2019MS002032 (2020).

41. Forster, P. et al. *Climate Change 2021: The Physical Science Basis. Contribution of Working Group I to the Sixth Assessment Report of the Intergovernmental Panel on Climate Change* (Cambridge University Press, 2021).

42. Shine, K. P., Fuglestvedt, J. S., Hailemariam, K. & Stuber, N. Alternatives to the global warming potential for comparing climate impacts of emissions of greenhouse gases. *Clim. Change* **68**, 281–302 (2005).

43. Myhre, G. D. et al. *Anthropogenic and Natural Radiative Forcing* (Cambridge University Press, Cambridge, United Kingdom and New York, 2013).

44. Collins, W. J., Frame, D. J., Fuglestvedt, J. S. & Shine, K. P. Stable climate metrics for emissions of short and long-lived species—combining steps and pulses. *Environ. Res. Lett.* **15**, 024018 (2020).

45. Etminan, M., Myhre, G., Highwood, E. J. & Shine, K. P. Radiative forcing of carbon dioxide, methane, and nitrous oxide: a significant revision of the methane radiative forcing. *Geophys. Res. Lett.* **43**, 12,614–12,623 (2016).

46. Fuglestvedt, J. S. et al. Metrics of climate change: assessing radiative forcings and emission indices. *Clim. Change* **58**, 267–331 (2003).

47. Shine, K. P., Berntsen, T. K., Fuglestvedt, J. S. & Sausen, R. Scientific issues in the design of metrics for inclusion of oxides of nitrogen in global climate agreements. *Proc. Natl. Acad. Sci. USA* **102**, 15758–15773 (2005b).

48. Allen, M. R. et al. New use of global warming potentials to compare cumulative and short-lived climate pollutants. *Nature Clim. Change* **6**, 773–777 (2016).

49. Frazer-Nash *Fugitive Hydrogen Emissions in a Future Hydrogen Economy* (Department of Business, Energy, and Industrial Strategy, United Kingdom, 2022).

50. Hydrogen Council. *Hydrogen Scaling up, a Sustainable Pathway for the Global Energy Transition.* https://hydrogencouncil.com/wp-content/uploads/2017/11/Hydrogen-scaling-up-Hydrogen-Council.pdf (2017).

51. Hydrogen Council. *Hydrogen Decarbonization Pathways, Potential Supply Scenarios.* https://hydrogencouncil.com/wp-content/uploads/2021/01/Hydrogen-Council-Report_Decarbonization-Pathways_Part−2_Supply-Scenarios.pdf (2021).

52. Boucher, O. & Reddy, M. S. Climate trade-off between black carbon and carbon dioxide emissions. *Energy Policy* **36**, 193–200 (2008).

53. International Energy Agency. *Net Zero By 2050.* (IEA, Paris, 2021). https://www.iea.org/reports/net-zero-by-2050.

54. Hydrogen Council. *Hydrogen for Net-Zero, a Critical Cost-Competitive Energy Vector.* https://hydrogencouncil.com/wp-content/uploads/2021/11/Hydrogen-for-Net-Zero_Full-Report.pdf (2021).

55. European Hydrogen Roadmap. A sustainable pathway for the European energy transition. *Fuel Cell and Hydrogen* https://www.fch.europa.eu/sites/default/files/Hydrogen%20Roadmap%20Europe_Report.pdf (2019).

56. TYNDP 2022. *Scenario report, ENTSOG & ENSTO-E. Brussels, Belgium* https://2022.entsos-tyndp-scenarios.eu/wp-content/uploads/2022/04/TYNDP2022_Joint_Scenario_Full-Report-April-2022.pdf (2022).

57. Collins, W. J. et al. Increased importance of methane reduction for a 1.5-degree target. *Environ. Res. Lett.* **13**, 054003 (2018).

58. Lewis, A. Optimising air quality co-benefits in a hydrogen economy: a case for hydrogen-specific standards for NOx emissions. *Environ. Sci. Atmos.* **1**, 201 (2021).

59. Tanaka, K., O'Neill, B. C., Rokityanskiy, D., Obersteiner, M. & Tol, R. S. J. Evaluating Global Warming Potentials with historical temperature. *Climatic Change.* **96**, 443–466 (2009).

60. Joos, F. & Bruno, M. Pulse response functions are cost-efficient tools to model the link between carbon emissions, atmospheric CO_2 and global warming. *Phys. Chem. Earth* **21**, 471–476 (1996).

61. Prather, M. J. Lifetimes and eigenstates in atmospheric chemistry. *Geophys. Res. Lett.* **21**, 801–804 (1994).

62. Fiore, A. M. et al. Multimodel estimates of intercontinental source-receptor relationships for ozone pollution. *J. Geophys. Res.* **114**, D04301 (2009).

63. Fuglestvedt, J. S. et al. Transport impacts on atmosphere and climate: metrics. *Atmos. Environ.* **44**, 4648–4677 (2010).

64. Terrenoire, E. et al. Impact of present and future aircraft NOx and aerosol emissions on atmospheric composition and associated direct radiative forcing of climate. *Atmos. Chem. Phys. Discuss.* https://doi.org/10.5194/acp-2022-222 (2022).

65. Boucher, O., Friedlingstein, P., Collins, B. & Shine, K. P. The indirect global warming potential and global temperature change potential due to methane oxidation. *Environ. Res. Lett.* **4**, 044007 (2009).

66. Geoffrey, O. et al. Transient climate response in a two-layer energy balance model. Part I: analytical solution and parameter calibration using CMIP5 AOGCM experiments. *J. Clim.* **26**, 1841–1857 (2013).

67. Lund, M. T. et al. A continued role of short-lived climate forcers under the Shared Socioeconomic Pathways. *Earth Syst. Dynam.* **11**, 977–993 (2020).

68. Gasser, T., et al. Accounting for the climate-carbon feedback in emission metric. *Earth Syst. Dyn.* **8**, 235–253 (2017).

69. Bloomberg NEF. *Hydrogen Economy Outlook, Key Messages.* https://data.bloomberglp.com/professional/sites/24/BNEF-Hydrogen-Economy-Outlook-Key-Messages-30-Mar-2020.pdf (2020).

70. Sun, P. et al. Criteria air pollutants and greenhouse gas emissions from hydrogen production in U.S. steam methane reforming facilities. *Environ. Sci. Technol.* **53**, 7103–7113 (2019).

71. Budsberg, E., Crawford, J., Gustafson, R., Bura, R. & Puettmann, M. Ethanologens vs. acetogens: Environmental impacts of two ethanol fermentation pathways. *Biomass and Bioenergy.* **83**, 23–31 (2015).

72. International Gas Union. *Natural Gas Conversion Guide* (International Gas Union, 2012).

Author contributions

D.H. originated the ideas, made the metric calculations, and led the writing of the paper with contributions from the coauthors M.S., F.P., R.D., W.C. and O.B. F.P. made the GFDL-AM4.1 simulations used as input to the metric calculations. W.C. calculated the uncertainties on the metrics.

Competing interests

The authors declare no competing interests.

Additional information

Supplementary information The online version contains supplementary material available at https://doi.org/10.1038/s43247-022-00626-z.

Correspondence and requests for materials should be addressed to Didier Hauglustaine.

Peer review information *Communications Earth & Environment* thanks the anonymous reviewers for their contribution to the peer review of this work. Primary Handling Editors: Nadine Mengis and Clare Davis. Peer reviewer reports are available.

Reprints and permission information is available at http://www.nature.com/reprints

Publisher's note Springer Nature remains neutral with regard to jurisdictional claims in published maps and institutional affiliations.